Available online at www.sciencedirect.com
ScienceDirect
Polymer 49 (2008) 992–998
polymer
www.elsevier.com/locate/polymer

Rate-dependence of yielding in ethylene–methacrylic acid copolymers

Robert C. Scogna, Richard A. Register*

Department of Chemical Engineering, Princeton University, Princeton, NJ 08544-5263, United States

Received 15 November 2007; received in revised form 31 December 2007; accepted 5 January 2008
Available online 11 January 2008

Abstract

It is well known that reducing the crystal thickness of polyethylene, by copolymerization with an α-olefin, decreases the yield stress. By contrast, incorporation of methacrylic acid (MAA) – also a noncrystallizable comonomer – results in a marked *increase* of the yield stress at room temperature at typical strain rates. We show that, in addition to crystal plasticity, one must consider the active mechanical relaxations to understand this phenomenon. For ethylene–methacrylic acid copolymers, the α and β relaxations are important over the range of conditions probed in this study, and the increase in the β relaxation (glass transition) temperature with MAA content is identified as the source of this peculiar behavior. The yield stress of these materials is adequately described by a model combining thermal nucleation of dislocations in the crystals with a Ree–Eyring dependence for yielding in the amorphous phase, all with physically reasonable parameter values. Yield stress master curves may be created from data taken at various temperatures and strain rates, and are presented herein for low-density polyethylene and five ethylene–methacrylic acid copolymers of varying MAA content.

Keywords: Ethylene copolymer; Yield stress; Mechanical relaxation

1. Introduction

Ethylene–methacrylic acid (E/MAA) copolymers were first developed over four decades ago and have since found widespread use both as copolymers and as their partially neutralized salts, otherwise known as ''ionomers''. Given their usefulness in mechanically demanding applications, it is quite surprising that the literature regarding the yield behavior of such materials is scarce [1]. These statistical E/MAA copolymers are chemically homogeneous and are formed in the same high-pressure, free-radical polymerization process that produces low-density polyethylene (LDPE). Therefore, in the limit of zero MAA content, their yield behavior should approach that of LDPE; polyethylene yield behavior has been studied extensively, though historically, two disparate approaches have been used. The first approach has been to assume that the yield stress can be modeled in terms of crystal slip alone: in other words, the contribution to the yield stress from the amorphous chain segments is assumed to be negligible. Shadrake and Guiu [2,3] developed an expression for the minimum tensile stress, σ_c, needed to thermally nucleate the [001] screw dislocations necessary for the (*hk*0)[001] slip system to be active in a polyethylene crystal of a given thickness, l_c. This expression predicts that the yield stress will increase monotonically with increasing crystal thickness, a prediction verified via experiment [4]. Though the free energy for the nucleation event is a function of shear rate [5], the rate-dependence is often ignored and a reasonable, constant value is assumed instead [6].

The second approach has been to model plastic deformation as a series of thermally activated rate processes, as suggested by Ree and Eyring [7]. The yield stress contribution from each process is assumed to be linearly additive. In most cases, only one or two processes are needed, even over broad ranges of temperature and strain rate. Each Ree–Eyring process generally corresponds to a relaxation process observed via dynamic mechanical spectroscopy. The Ree–Eyring model has found great utility in describing the yield behavior of amorphous and slightly crystalline polymers such as poly(methyl methacrylate) [8] and poly(vinyl chloride) [9], as well as a few highly

* Corresponding author. Tel.: +1 609 258 4691; fax: +1 609 258 0211.
E-mail address: register@princeton.edu (R.A. Register).

0032-3861/$ - see front matter © 2008 Elsevier Ltd. All rights reserved.
doi:10.1016/j.polymer.2008.01.005

crystalline polymers such as isotactic polypropylene [10] and high-density polyethylene [11]. Another interesting feature of this model is that superposition of yield stress data taken at various temperatures is possible [9], using horizontal and vertical shifts which are coupled: that is, they are constrained by the form of the Ree–Eyring equation. The superposition method allows for the creation of a master curve which describes the yield stress of a material over a broad range of temperatures and strain rates. Herein, we combine the models for crystal slip and activated rate processes to elucidate the microstructural processes which are important in the yielding of E/MAA copolymers at various temperatures and strain rates.

2. Experimental section

2.1. Materials

LDPE ($\rho = 0.923$ g/cm^3) and E/MAA copolymers were provided by DuPont Packaging and Industrial Polymers. These copolymers ranged in composition from 4 to 19 wt% MAA (1.3–7.1 mol% MAA) [12]. The sample code (e.g., E/6MAA) indicates the content of the acid comonomer (6MAA = 6 wt% MAA). The copolymer pellets were melt-pressed into 0.2–0.5 mm thick sheets at 140–150 °C in a PHI hot press. The samples were then stored in a desiccator at room temperature for at least one week. ASTM D1708 dogbones with a gauge length of 22 mm were stamped from these sheets for tensile testing. Copolymer pellets were also pressed into sheets of 0.1 mm thickness for dynamic mechanical thermal analysis (DMTA), for which the sample dimensions were approximately 5×22 mm^2.

2.2. Characterization

Uniaxial tensile stress–strain curves, at temperatures ranging from 0 to 35 °C, were obtained with an Instron Model 5865, equipped with an Environmental Chamber 3111 retrofitted to control the testing temperature to within 0.3 °C with a cycle time of 1 s. Subambient temperatures were achieved by introducing a small quantity of dry ice into the chamber. Samples were allowed to thermally equilibrate for at least 5 min. The crosshead speeds employed ranged from 8.5×10^{-3} to 8.5 mm/s, producing engineering strain rates of 3.8×10^{-4} to 3.8×10^{-1} s^{-1}. DMTA measurements were performed at 1 Hz on a TA Instruments RSA 3, using the film fixture. Data were collected every 5 °C for an effective heating rate of about 10 °C/min.

3. Results and discussion

3.1. Yield point determination

Tensile tests of the LDPE and E/MAA copolymers were performed at various temperatures and strain rates. At sufficiently high strain rates and low temperatures, all polymers showed a local maximum in stress at the yield point. This local maximum corresponded with the initiation of a shallow neck in the tensile test sample. However, at sufficiently low strain rates and high temperatures, neither a local maximum nor necking was observed; extension was homogeneous throughout the gauge length. To consistently determine the yield stress regardless of the presence or absence of necking, the yield stress was taken as the stress exerted on the sample at a strain that corresponds to the intersection of the Young's modulus line and a line fit to the pseudo-linear region immediately following the yield point. Fig. 1 depicts this scheme for the 0.38 s^{-1} strain rate tensile test. This method roughly corresponds to the strain offset method of yield point determination if an offset of 1% is employed. At these strains (<10%), no permanent plastic deformation is observed; indeed, as is known for low-density polyethylenes [13], strains well beyond this initial yield point are required before irrecoverable deformation sets in. Note that engineering yield stresses are reported here, as opposed to true stresses, since the yield strain magnitude is small and does not change substantially with strain rate, as demonstrated in Fig. 1. The yield stress decreases with decreasing strain rate, as expected.

3.2. Yield stress model

In the limit of very low strain rates, amorphous-phase processes should be completely relaxed. In this regime, the only resistance to deformation comes from crystal slip. Following Shadrake and Guiu [2,3], the minimum tensile stress, σ_c, necessary for crystal plasticity via an (hk0)[001] slip system is,

$$\sigma_c = \frac{K(T)\mathrm{B}}{\pi r_o} \exp\left[\frac{-2\pi\Delta G^*}{K(T)\mathrm{B}^2 l_c} - 1\right], \quad (1)$$

where $K(T)$ is the temperature-dependent shear modulus of the slip plane, for which we employed the simulation results of Karasawa et al. [14], B is the magnitude of the Burgers vector,

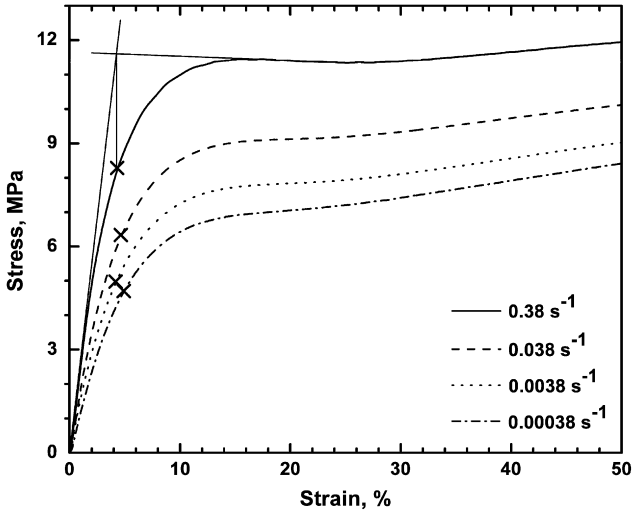

Fig. 1. Yield regime for E/6MAA, at four different strain rates, all at 22 °C. Note the absence of a local maximum in stress as the strain rate decreases. The Young's modulus and post-yield linear fit lines are shown for the 0.38 s^{-1} curve to demonstrate the method for yield point determination. The yield point (×) for tests conducted at lower $\dot{\varepsilon}$ is also shown.

r_o is the dislocation core radius, l_c is the crystal thickness, and ΔG^* is the energy barrier for the nucleation event. Some researchers [6,15] choose a constant value for ΔG^*, typically between $40kT$ and $60kT$. However, Crist [5] suggested that crystal plasticity is an activated process, and ΔG^* may accordingly be defined as,

$$\Delta G^* = -kT \ln\left(\frac{\dot{\varepsilon}}{\dot{\varepsilon}_c}\right). \tag{2}$$

Thus, the factor of 40–60 is replaced by a strain-rate-dependent quantity, $-\ln(\dot{\varepsilon}/\dot{\varepsilon}_c)$, where $\dot{\varepsilon}_c$ characterizes the rate of segmental motion. While $\dot{\varepsilon}_c$ in principle represents a microscopic frequency factor for segmental motion, we simply set $\dot{\varepsilon}_c = 10^{18}\ s^{-1}$ here, so as to obtain $\Delta G^*/kT$ values within the physically reasonable range [16] of 40–50 over the range of strain rates we employ. The Burgers vector magnitude B is assumed to be equal to the polyethylene *c*-axis dimension [5] of 0.254 nm. The dislocation core radius for a (100)[001] screw dislocation in polyethylene comes from computer simulations [17] and is equal to 1.0 nm. The crystal thickness can thus be extracted from experimental data by applying Eq. (1) to the low-$\dot{\varepsilon}$ regime of the higher-temperature data sets, where the contribution from amorphous-phase mechanical relaxations is negligible.

As the strain rate increases, the contribution of amorphous-phase relaxation processes can no longer be ignored. The contribution from each relaxation process may be represented as a term in the Ree–Eyring model [7],

$$\frac{\sigma_{re}}{T} = \sum_i \frac{R}{v_i} \sinh^{-1}\left[\frac{\dot{\varepsilon}}{\dot{\varepsilon}_{0,i}} \exp\left(\frac{\Delta H_i}{RT}\right)\right], \tag{3}$$

where σ_{re} is the tensile stress contribution from "i" relaxation processes, R is the gas constant, v_i is the activation volume, $\dot{\varepsilon}$ is the applied strain rate, $\dot{\varepsilon}_{0,i}$ is a constant pre-exponential factor and ΔH_i is the activation energy.

We begin by assuming that the yield stress of the LDPE and E/MAA copolymers may be described by the simple addition of these crystalline and amorphous contributions to yield,

$$\frac{\sigma_y}{T} = \frac{\sigma_c}{T} + \frac{\sigma_{re}}{T}, \tag{4}$$

where σ_y is the yield stress and σ_c and σ_{re}/T are given by Eqs. (1) and (3), respectively. This assumption implies that the strain in both the amorphous and crystalline regions is identical, as expected for the usual morphological model, consisting of crystalline lamellae stacked along the *c*-axis direction and separated by amorphous layers. If the yield stress normalized by temperature is plotted against the logarithm of the strain rate, each relaxation process will appear to dominate over some range of strain rates, where this process is no longer relaxed and plays a significant role in the measured yield behavior. Fig. 2 illustrates how a system that follows Eq. (4) breaks down into its respective parts, assuming that only one Eyring process is needed (i.e., $i = 1$ in Eq. (3)). Note the relatively weak dependence of the crystal slip contribution on strain rate, as described by Eq. (2).

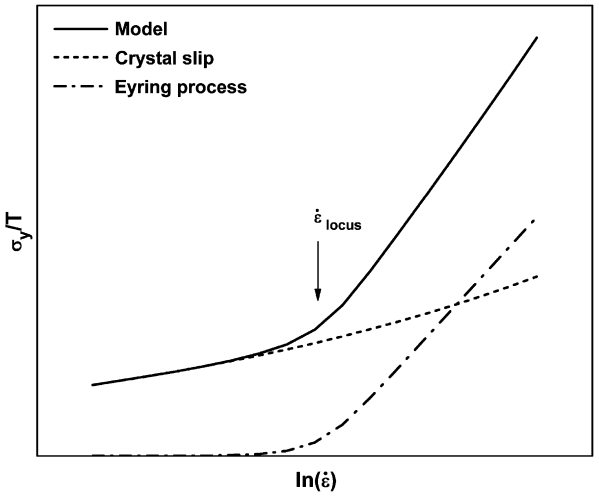

Fig. 2. Schematic showing the relative contributions from rate-dependent crystal slip and a single Eyring process, combined into a single model as described in the text.

The experimentally-determined yield stress for E/6MAA was normalized by the absolute temperature and plotted against the logarithm of the strain rate. Care was taken never to exceed 35 °C, as this could cause the thin, secondary crystals to melt [18]. The results are shown in the left panel of Fig. 3. There appear to be two asymptotes: one at low strain rates and one at high strain rates. This supports the notion that two microstructural processes are relevant over the range of conditions studied. Similar to the work of Bauwens-Crowet [9], horizontal and vertical shift factors, s_x and s_y, may be derived; these allow data sets taken at various temperatures, T, to be superimposed to create a master curve at a reference temperature of T_{ref}.

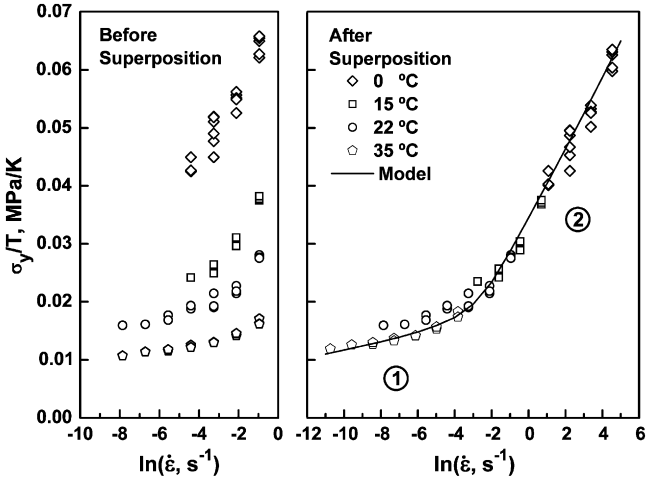

Fig. 3. Left: yield stress at various strain rates, at the temperatures indicated. Right: master curve formed from the data via the shift factors given by Eq. (5)–(7), with the best-fit parameter values in Table 1. Solid line shows the calculated model fit according to Eq. (4); crystal plasticity dominates in regime 1, while incomplete amorphous-phase relaxation dominates the yield stress in regime 2.

$$s_x = \frac{-\Delta H}{R}\left(\frac{1}{T_{\mathrm{ref}}} - \frac{1}{T}\right), \tag{5}$$

$$s_y = \frac{\sigma_c\left(T_{\mathrm{ref}}, \dot{\varepsilon}_{\mathrm{locus},T_{\mathrm{ref}}}\right)}{T_{\mathrm{ref}}} - \frac{\sigma_c\left(T, \dot{\varepsilon}_{\mathrm{locus},T}\right)}{T}, \tag{6}$$

where,

$$\dot{\varepsilon}_{\mathrm{locus},T} = \frac{\dot{\varepsilon}_0}{2\exp(\Delta H/RT)}, \tag{7}$$

$\sigma_c(T_{\mathrm{ref}})$ and $\sigma_c(T)$ are the contributions from crystal slip, given by Eq. (1), evaluated at T_{ref} and T, respectively. In this work, T_{ref} is chosen to be 22 °C (295 K). Since only one Eyring process is needed, the subscript "1" from Eq. (3) has been omitted for clarity. Eq. (5) for the horizontal shift factor s_x is a simple Arrhenius expression, with an activation energy ΔH for the Eyring process. However, as discussed by Bauwens-Crowet [9], the fact that two processes are operative, each with its own activation energy (Eyring process in Eq. (5), crystal slip in Eq. (2)), mandates a corresponding vertical shift s_y as well, given by Eq. (6). $\dot{\varepsilon}_{\mathrm{locus}}$, appearing in Eq. (6) and defined in Eq. (7), is the strain rate at the crossover between the two processes, measured as the linear extrapolation of the high-rate Eyring process to where it intersects the low-rate crystal slip process (indicated graphically in Fig. 2). $\dot{\varepsilon}_{\mathrm{locus}}$ is naturally temperature-dependent, as the position of the crossover shifts along both the abscissa ($\dot{\varepsilon}$) and the ordinate (σ_y/T) as temperature changes. The Levenberg-Marquardt algorithm was used to determine the best-fit parameter values for v, ΔH, and $\dot{\varepsilon}_0$, listed in Table 1. These parameter values result in the superposition of E/6MAA yield data shown in the right panel of Fig. 3.

The superposition process was repeated for the 11.5, 15 and 19 wt% MAA copolymers. The resulting model fits and associated parameter values are shown in Fig. 4 and Table 1, respectively. The behavior of the higher-MAA copolymers is similar to that of the E/6MAA copolymer: at lower strain rates (or, equivalently, higher temperatures), there exists a low-slope regime while, at higher rates (or lower temperatures), the slope increases dramatically. However, as the MAA content increases from 11.5 to 19 wt%, the strain rate at which the high-slope regime begins decreases, indicating a shift of $\dot{\varepsilon}_{\mathrm{locus}}$ to smaller values. Such a shift is expected if the amorphous-phase relaxation slows with increased MAA content. In support of this idea, Fig. 5 shows the loss modulus, E'', from −60 to 60 °C for these three copolymers, showing a progressive increase in the temperature of the relaxation with MAA content, in good quantitative agreement with prior

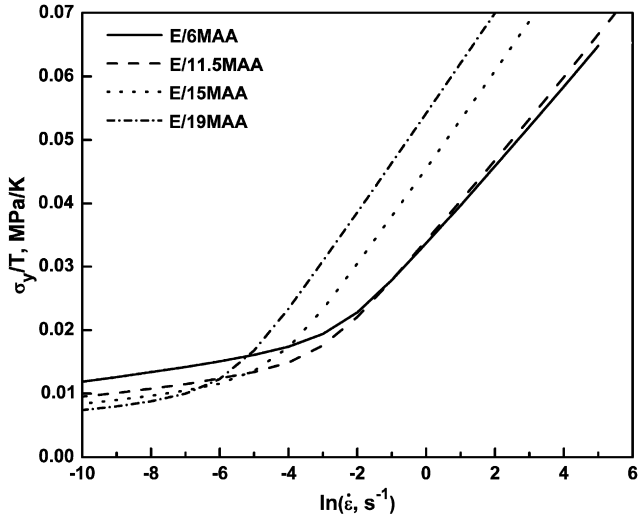

Fig. 4. Comparison of master curves, all with $T_{\mathrm{ref}} = 22$ °C, for 6, 11.5, 15 and 19 wt% MAA copolymers. Data points are omitted to preserve legibility.

DMTA measurements on these same polymers [12]. If the peak in the E/MAA β relaxation is taken as the glass transition temperature T_g, then the T_g values of E/11.5MAA, E/15MAA and E/19MAA are 1, 10, and 19 °C, respectively. As the copolymer T_g approaches room temperature, both ΔH and $\dot{\varepsilon}_0$ increase substantially, as expected in fitting a glass transition process to the simple Arrhenius expression of Eq. (5). The ΔH value of 226 kJ/mol for E/11.5MAA, shown in Table 1, is in excellent agreement with the E/MAA β relaxation value of 234 kJ/mol [19] for a copolymer of identical MAA content, as determined by dielectric spectroscopy. Additionally, the activation volumes for these copolymers are typical of glassy polymers [20]. Thus, for moderate to high MAA content copolymers, the high-slope regime at high strain rates and/or low temperatures (regime 2 in Fig. 3) is attributed to the E/MAA β transition. Indeed, the rising temperature of the β transition has already been identified as the cause of similarly peculiar behavior of the Young's modulus in these materials, where increased MAA content can actually raise the modulus while simultaneously lowering the crystallinity [12].

However, at very low MAA contents, both the relaxation and yield behavior become more complex. Fig. 6 shows that LDPE exhibits both a polyethylene β relaxation peak (at −24 °C) and a higher-temperature shoulder caused by the α relaxation (around 30 °C). The α relaxation is typically attributed to twisting of polyethylene chain segments within a polyethylene crystal [21]. According to Popli et al. [22], the polyethylene α and β processes merge into a single peak (which, to avoid confusion, is referred to here as the

Table 1
Model best-fit parameter values with 95% confidence intervals

	E/0MAA	E/4MAA	E/6MAA	E/11.5MAA	E/15MAA	E/19MAA
l_c, nm	3.2	3.0	2.9	2.7	2.6	2.5
v, nm^3	5.0 ± 0.3	3.3 ± 0.3	2.9 ± 0.2	2.7 ± 0.1	2 ± 1	2.0 ± 0.6
ΔH, kJ/mol	120 ± 10	100 ± 10	170 ± 10	226 ± 2	210 ± 2	219 ± 2
$\log_{10}(\dot{\varepsilon}_0, \mathrm{s}^{-1})$	20 ± 3	18 ± 3	29 ± 3	39 ± 3	35 ± 4	36 ± 4

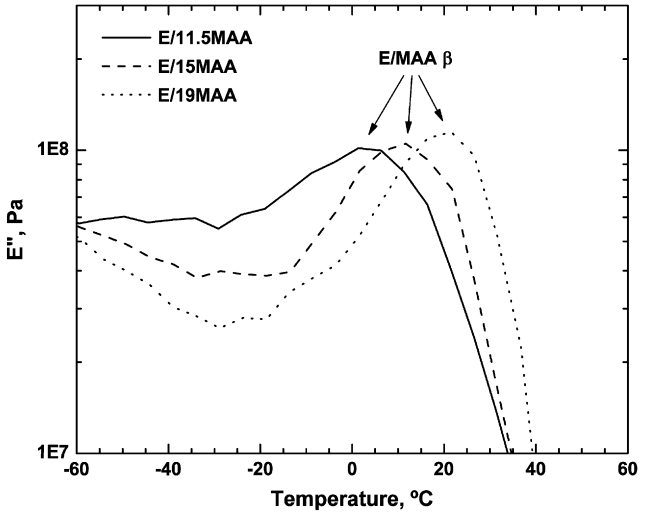

Fig. 5. DMTA data at 1 Hz for copolymers of moderate to high MAA content. Note the increase in T_β with increasing MAA content.

β relaxation for E/MAA copolymers) if the polyethylene crystals are sufficiently thin. Since MAA units are excluded from the polyethylene crystals, it is expected that as the MAA content is reduced towards LDPE (zero MAA), the crystals will become thicker, and the α and β relaxations will gradually separate. This emergence of the α relaxation in Fig. 6 is reflected in the yield stress master curve for LDPE shown in Fig. 7. In "regime 2", at reduced strain rates of $\ln \dot{\varepsilon} = -4$ and higher, the slope of the LDPE yield data is significantly lower than that for the E/6MAA copolymer shown again for comparison. The literature shows that ΔH for the LDPE α relaxation is roughly 100 kJ/mol [21], which is close to the $\Delta H = 120$ kJ/mol obtained for LDPE from our model fit (Table 1). Thus, the "regime 2" observed in Fig. 7 for LDPE corresponds to the α relaxation; a third region of even steeper slope would be expected at higher $\dot{\varepsilon}$, where the LDPE β process is no

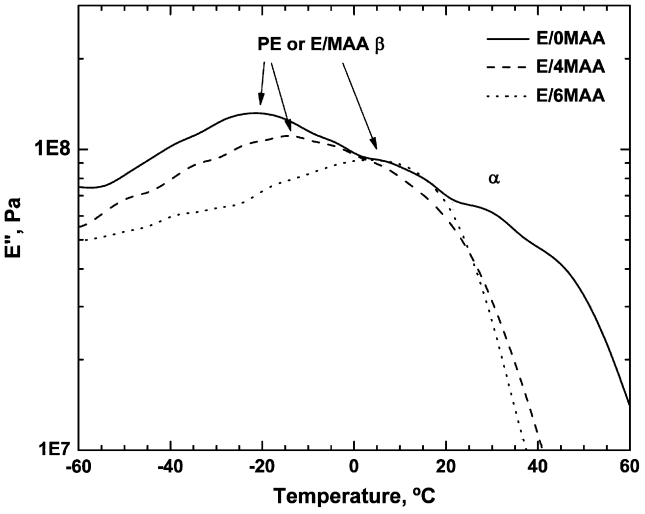

Fig. 6. DMTA data at 1 Hz for copolymers with low to moderate MAA content. Note the shoulder present in the LDPE data near 30 °C due to the α relaxation. As the MAA content is increased, this shoulder merges with the β relaxation to form a single peak.

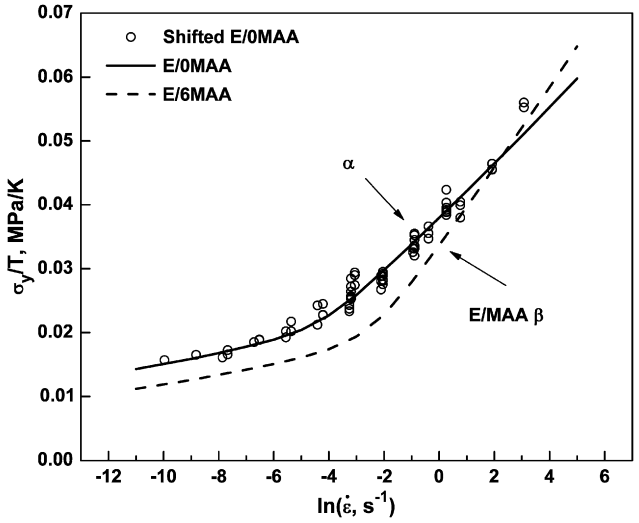

Fig. 7. Comparison of the LDPE and E/6MAA master curves, both with $T_{ref} = 22$ °C. The high strain rate "regime 2" for LDPE has a lower slope than for the E/6MAA copolymer, as it corresponds to incomplete relaxation of the LDPE α process.

longer completely relaxed. The points at the highest $\dot{\varepsilon}$ in Fig. 7 hint at such a region, but additional data at even lower temperatures would be required for a thorough assessment, given the low LDPE $T_\beta = -24$ °C.

Fig. 4 also shows that, in the low-rate limit, σ_c decreases monotonically with increasing comonomer content. This is expected from Eq. (1): increasing MAA content should yield thinner crystals, a trend captured in the values of l_c extracted from the model fits (Table 1). However, E/MAA copolymers are known to have a bimodal distribution of crystal thickness, with primary crystals of thickness ≈6 nm, and secondary crystals of thickness ≈3 nm [18]. Though the values of l_c listed in Table 1 are close to 3 nm, it does not seem plausible that the secondary crystals could dominate the response of the crystalline phase. While the model fit value of l_c is expected to reflect some average of these two populations, it must be strongly weighted in favor of the thicker primary crystals; otherwise, the model would predict that raising the temperature enough to melt the thin secondary crystals would increase σ_y, which is inconsistent with experiment. Thus, it appears that the values of l_c determined by the model are simply too small, by a factor of ≈2. However, recall that the values of l_c are extracted from the measured values of σ_c via Eq. (1), so their numerical values depend on the other parameters employed in the evaluation of Eq. (1). In particular, the shear modulus, $K(T)$, deserves further consideration; its value is extremely sensitive to the unit cell parameters of the crystal, as these strongly influence the interaction energies between lines of atoms [23]. $K(T)$, equal to $\sqrt{C_{44}C_{55}}$, is often determined by atomistic simulation, where the thickness of the periodic crystal is effectively infinite [24–28]. But in the thin crystals which form in ethylene copolymers, the a and b lattice parameters can increase by 1–2% to ameliorate packing-induced stresses at the crystal surfaces [29]. Using an analytical approach [23], we estimate that 1–2% increases in a and

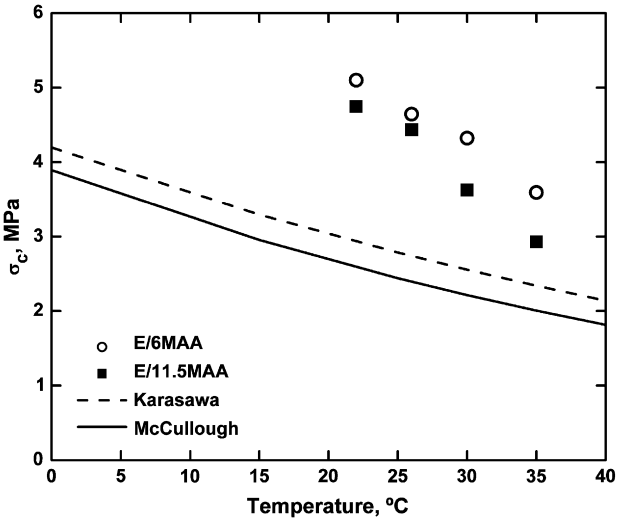

Fig. 8. Experimentally-determined temperature dependence of σ_c for E/6MAA and E/11.5MAA (at a low strain rate of 3.8×10^{-3} s^{-1}, where the E/MAA β process is completely relaxed) vs. the σ_c predicted using $K(T)$ given by Karasawa [13] (also used by Brooks [30]) and by McCullough [23] with $l_c = 2.5$ nm.

b can decrease $K(T)$ by 30%, leading to a twofold *increase* in the value of l_c extracted from Eq. (1). Thus, the small values of l_c listed in Table 1 may simply reflect uncertainties in the precise values of K which apply for the thin polyethylene crystals in these copolymers.

Close inspection of Figs. 3 and 7 reveals that while the superposition of the yield data is generally quite good, there appears to be some mismatch at the low strain rates where σ_c is evaluated. The most likely explanation for this is a mismatch between the temperature dependence of K assumed in the model, and the experimental temperature dependence of σ_c (σ_y at low strain rates). Unfortunately, C_{44} and C_{55} are rarely given as functions of temperature, with only two such studies published [13,23]. Fig. 8 shows experimentally-determined σ_c values for E/6MAA and E/11.5MAA, compared with σ_c values predicted by Eq. (1) using the two $K(T)$ functions reported from simulations; the experimental σ_c decreases roughly two to three times faster with temperature than predicted. While the reason for this discrepancy is not yet clear, it has been previously observed [5].

4. Conclusions

The yield stress of E/MAA copolymers can be described by the simple sum of the contributions from crystal slip and other mechanical relaxations, such as the polyethylene α and β transitions. The crystal slip contribution can be described by the model of Shadrake and Guiu [2,3] while mechanical relaxations are incorporated through the Ree–Eyring treatment [7]. The combined model was fit to yield stress data for LDPE and five E/MAA copolymers of varying MAA content. Superposition of the yield data using coupled horizontal and vertical shifts was used to generate a master curve for each material; superposition was good, though there was a small amount of mismatch at low strain rate, attributed to the relatively weak temperature dependence of the shear modulus, K, predicted by simulation and utilized as an input in the model. The crystal thicknesses extracted from the model decrease as the MAA content increases, as expected.

DMTA on moderate to high MAA content copolymers revealed a single peak in E'', over the range of temperatures studied, corresponding to the E/MAA β relaxation. At high strain rates (regime 2 in Fig. 3), the E/MAA β relaxation was not fully relaxed. As a consequence, the yield stress rose quite quickly as the strain rate increased. The ΔH value for this regime, obtained from the model fit, was in good agreement with E/MAA β relaxation ΔH values in the literature. The fitted activation volumes for these copolymers are quite reasonable for a polymer below its T_g. At low MAA contents, the E/MAA β relaxation splits into two parts: the polyethylene α and β relaxations. The appearance of a separate α transition impacts the dependence of yield stress on strain rate: the slope is decidedly lower in regime 2 as compared to copolymers of high MAA content, and the ΔH value found for this regime agrees with literature values for the polyethylene α relaxation.

Acknowledgements

This work was generously supported by DuPont Packaging and Industrial Polymers, Sabine River Works. The authors thank Dr. George Prejean of DuPont for providing some of the materials studied herein, and for helpful discussions throughout.

References

[1] Rees RW, Vaughan DJ. Polym Prepr Am Chem Soc Div Polym Chem 1965;6:296–303.
[2] Shadrake LG, Guiu F. Philos Mag 1976;34:565–81.
[3] Shadrake LG, Guiu F. Philos Mag A 1979;39:785–96.
[4] Darras O, Séguéla R. J Polym Sci Part B Polym Phys 1993;31:759–66.
[5] Crist B. Plastic deformation of polymers. In: Cahn RW, Haasen P, Kramer EJ, editors. Materials science and technology: a comprehensive treatment. New York: VCH Publishers Inc.; 1993. p. 427–69.
[6] Séguéla R, Gaucher-Miri V, Elkoun S. J Mater Sci 1998;33:1273–9.
[7] Ree T, Eyring H. J Appl Phys 1955;26:793–800.
[8] Roetling JA. Polymer 1965;6:311–7.
[9] Bauwens-Crowet C, Bauwens JC, Homès G. J Polym Sci Part A2 1969;7:735–42.
[10] Roetling JA. Polymer 1966;1:303–6.
[11] Truss RW, Clarke PL, Duckett RA, Ward IM. J Polym Sci Polym Phys Ed 1984;22:191–209.
[12] Wakabayashi K, Register RA. Polymer 2005;46:8838–45.
[13] Brooks NW, Duckett RA, Ward IM. Polymer 1992;33:1872–80.
[14] Karasawa N, Dasgupta S, Goddard WA. J Phys Chem 1991;95:2260–72.
[15] Young RJ. Mater Forum 1988;11:210–6.
[16] Crist B, Fisher CJ, Howard PR. Macromolecules 1989;22:1709–18.
[17] Bacon DJ, Tharmalingham K. J Mater Sci 1983;18:884–93.
[18] Loo Y-L, Wakabayashi K, Huang YE, Register RA, Hsiao BS. Polymer 2005;46:5118–24.
[19] Phillips PJ, MacKnight WJ. J Polym Sci Part A2 1970;8:727–38.
[20] Haward RN, Thackray G. Proc R Soc A 1968;302:453–72.
[21] Boyd RH. Polymer 1985;26:1123–33.
[22] Popli R, Glotin M, Mandelkern L, Benson RS. J Polym Sci Polym Phys Ed 1984;22:407–48.

[23] McCullough RL, Peterson JM. J Appl Phys 1973;44:1224–30.
[24] Lacks DJ, Rutledge GC. J Phys Chem 1994;98:1222–31.
[25] Crist B, Hereña PG. J Polym Sci Part B Polym Phys 1996;34:449–57.
[26] Martoňák R, Paul W, Binder K. J Chem Phys 1997;106:8918–30.
[27] Tashiro K. Comput Theor Polym Sci 2001;11:357–74.
[28] Barrera GD, Parker SF, Ramirez-Cuesta AJ, Mitchell PCH. Macromolecules 2006;39:2683–90.
[29] Howard PR, Crist B. J Polym Sci Part B Polym Phys 1989;27:2269–82.
[30] Brooks NWJ, Duckett RA, Ward IM. J Polym Sci Part B Polym Phys 1998;36:2177–89.